Supplemental Figures

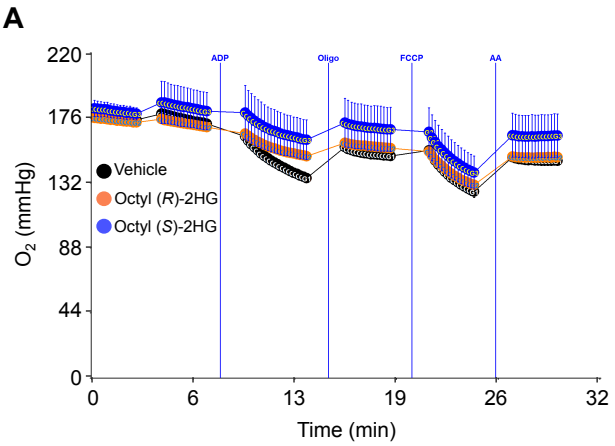

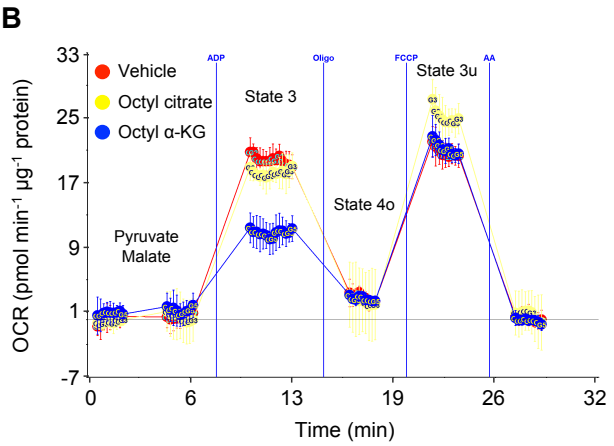

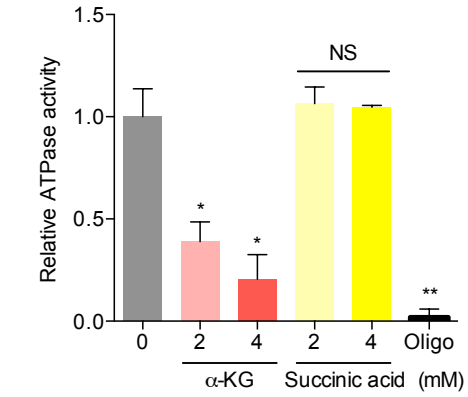

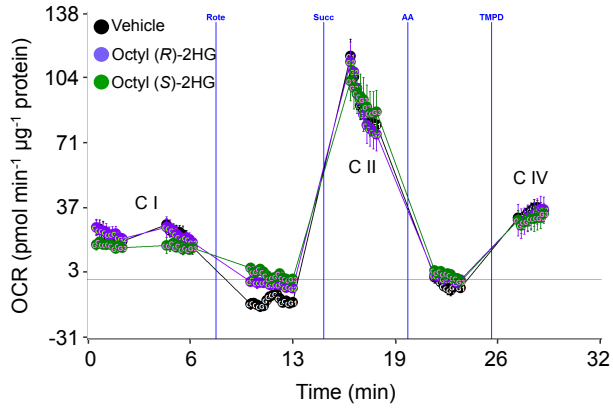

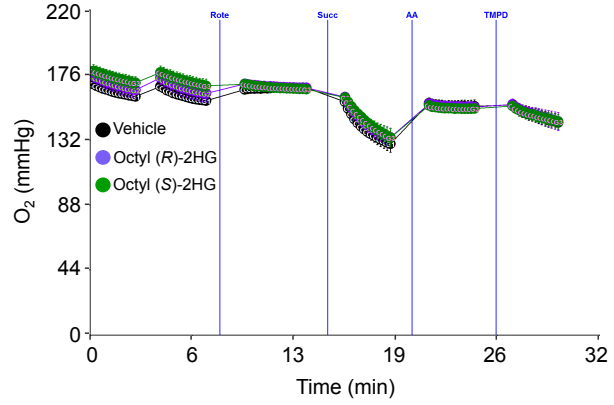

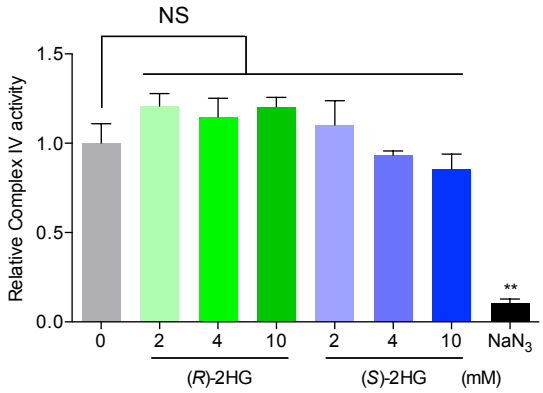

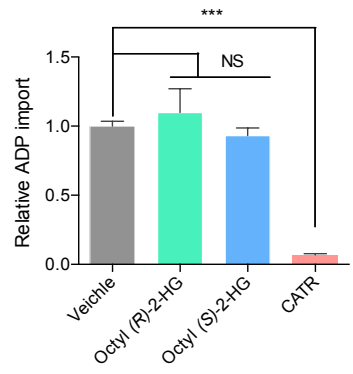

Figure S1, related to Figure 2. 2-HG does not affect the electron flow through the electron transport chain and does not affect ADP import

(A) Kinetic graphs of oxygen tension for Complex II coupling assay shown in Figure 2B, indicating that oxygen is not limiting in the assay.

(B) Octyl citrate (600 μM) has no effect on mitochondrial respiration and serves as a negative control for octyl 2-HG in Figure 2B; octyl α-KG (Chin et al., 2014) serves as a positive control.

(C) Inhibition of submitochondrial particle ATPase activity by α-KG acid and not by succinic acid (*P < 0.05, **P < 0.01; NS, P > 0.05; unpaired t-test, two-tailed, two-sample unequal variance). Oligo, oligomycin (32 μM). Mean ± s.d. is plotted.

(D) OCR from isolated mouse liver mitochondria at basal (pyruvate and malate as Complex I substrates, in presence of FCCP) and in response to sequential injection of rotenone (Rote; Complex I inhibitor), succinate (Complex II substrate), antimycin A (AA; complex III inhibitor), tetramethylphenylenediamine (TMPD; cytochrome c (Complex IV) substrate). No difference in Complex I (C I), Complex II (C II), or Complex IV (C IV) respiration is observed after 30 min treatment with 600 μM of octyl 2-HG, whereas Complex V is inhibited (Figure 2B) by the same treatment (2 independent experiments). Octanol is used as vehicle.

(E) Kinetic graphs of oxygen tension for the electron flow assay shown in (D), indicating that oxygen is not limiting in the assay.

(F) 2-HG does not inhibit Complex IV (NS, P > 0.05). NaN_3 (5 mM), a known Complex IV inhibitor, is used as positive control (**P = 0.0037; unpaired t-test, two-tailed, two-sample unequal variance). Mean ± s.d. is plotted.

(G) ADP import was measured in the presence of octanol (vehicle control) or octyl 2-HG (600 μM). Octyl *(R)*-2HG, P = 0.4237; octyl *(S)*-2HG, P = 0.1623. CATR (carboxyatractyloside, 10 μM), a known inhibitor for ADP import, was used as a positive control for the assay (***P = 0.0003). By unpaired t-test, two-tailed, two-sample unequal variance. Mean ± s.d. is plotted in all cases.

(A-G) Results were replicated in at least two independent assays.

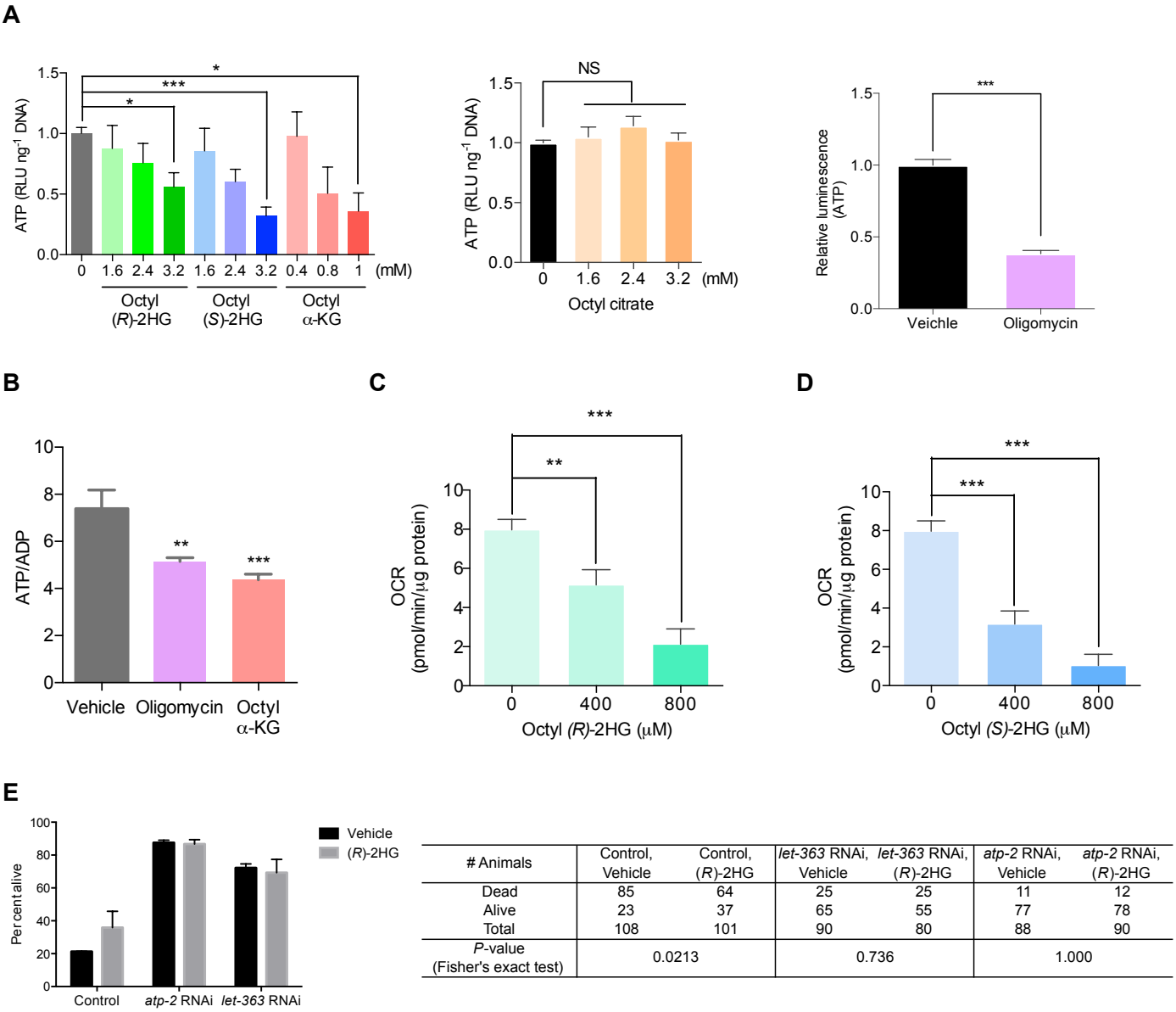

# Animals	Control, Vehicle	Control, (*R*)-2HG	*let-363* RNAi, Vehicle	*let-363* RNAi, (*R*)-2HG	*atp-2* RNAi, Vehicle	*atp-2* RNAi, (*R*)-2HG
Dead	85	64	25	25	11	12
Alive	23	37	65	55	77	78
Total	108	101	90	80	88	90
P-value (Fisher's exact test)	0.0213		0.736		1.000	

Figure S2, related to Figure 2. 2-HG inhibits cellular respiration and decreases ATP levels

(A) Decreased ATP content in U87 cells treated with octyl 2-HG or octyl α-KG (**P* < 0.05, ****P* < 0.001), but not with octyl citrate (NS, *P* > 0.05). Oligomycin (5 μM), a known inhibitor of ATP synthase, is used as a positive control. Octanol has no effect on ATP content.

(B) Octyl α-KG (800 μM) decreases ATP/ADP ratio. Oligomycin (5 μM) is a positive control. ***P* < 0.01, ****P* < 0.001.

(C-D) U87 cells treated with octyl 2-HG have decreased ATP synthase dependent (oligomycin sensitive) oxygen consumption rate (OCR) (***P* < 0.01, ****P* < 0.001).

By unpaired *t*-test, two-tailed, two-sample unequal variance.

(E) 2-HG longevity is mediated through ATP synthase and TOR. *atp-2* and *let-363* are the *C. elegans* homologs of ATP5B and TOR, respectively. Percent alive at day 19 of adulthood is plotted. **P* < 0.05, by Fisher's exact test, two-tailed.

(A-E) Results were replicated in at least two independent assays. Mean ± s.d. is plotted in all cases.

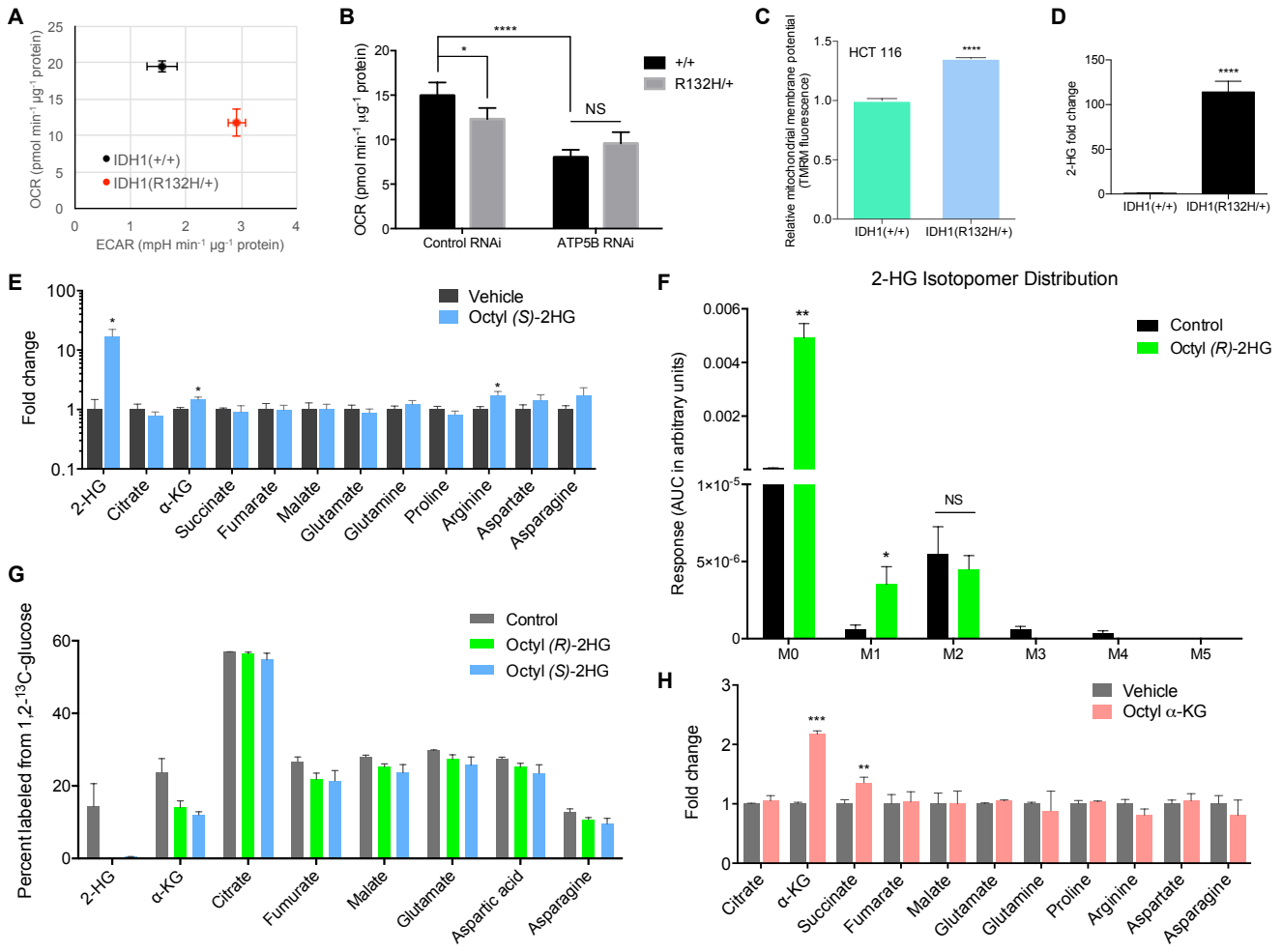

Figure S3, related to Figure 3. Cellular energetics and metabolic profiles of 2-HG accumulated cells

(A) HCT 116 IDH1(R132H/+) cells exhibit decreased respiration (***P* = 0.0015).

(B) Decreased respiration in HCT 116 IDH1(R132H/+) cells is ATP synthase dependent (**P* = 0.01; *****P* < 0.0001; NS, *P* = 0.0868).

(C) HCT 116 IDH1(R132H/+) cells exhibit increased mitochondrial membrane potential (*****P* < 0.0001); data were normalized to cell number.

(D) 2-HG levels are ~100 folder higher in HCT 116/IDH1(R132H/+) cells than in parental control cells (*****P* < 0.0001).

(E) Metabolic profile of TCA cycle intermediates and related amino acids in octyl *(S)*-2HG treated U87 cells (**P* < 0.05).

(F) 2-HG isotopomer distribution in cells cultured in medium containing 1,2-^{13}C-glucose. ***P* = 0.0039, **P* = 0.0407; NS, *P* = 0.4399.

(G) Percentage of labeled metabolites in cells cultured in medium containing 1,2-^{13}C-glucose. By unpaired *t*-test, two-tailed, two-sample unequal variance. Mean ± s.d. is plotted in all cases. Oligomycin has been reported to affect the total glucose contribution to citrate (Fendt et al., 2013). Since oligomycin inhibits the F_O subunit whereas 2-HG (and α-KG) targets the F_1 subunit, it is not likely that they will confer completely the same effects. Different levels of ATP synthase inhibition by α-KG, oligomycin, and genetic alterations are also known to elicit similar but non-identical phenotypes (Chin *et al.*, 2014).

(H) Metabolic profile of TCA cycle intermediates and related amino acids in octyl α-KG treated HEK 293 cells (***$P < 0.001$, **$P < 0.01$).
(A-G) Results were replicated in two independent experiments; (H) results were obtained from three biological replicates in one experiment.

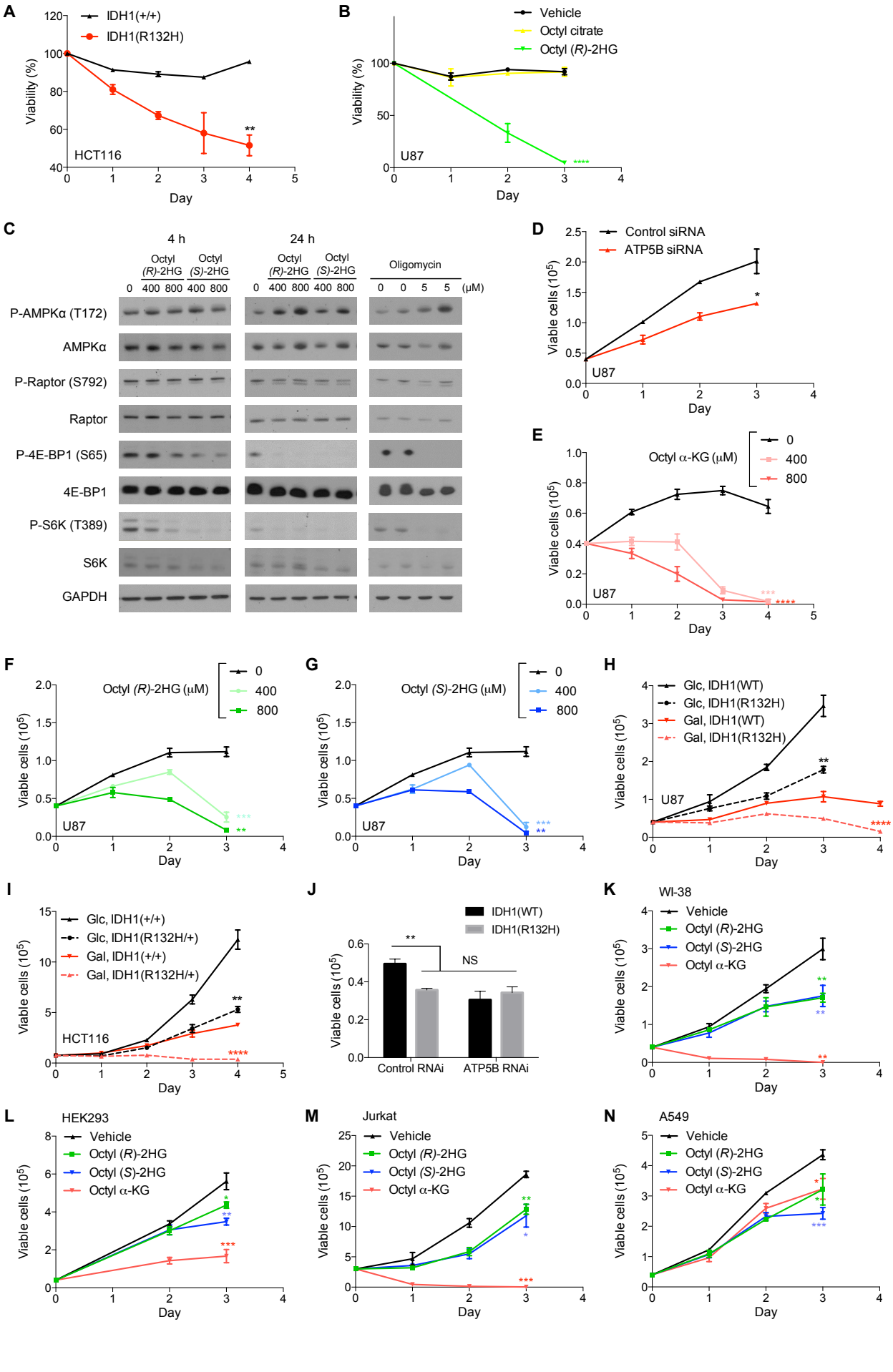
A
IDH1(+/+)
IDH1(R132H)
Viability (%)
HCT116
Day
B
Vehicle
Octyl citrate
Octyl (R)-2HG
U87
C
4 h
24 h
Octyl (R)-2HG
Octyl (S)-2HG
Oligomycin
0 400 800 400 800 0 400 800 400 800 0 0 5 5 (μM)
P-AMPKα (T172)
AMPKα
P-Raptor (S792)
Raptor
P-4E-BP1 (S65)
4E-BP1
P-S6K (T389)
S6K
GAPDH
D
Control siRNA
ATP5B siRNA
Viable cells (10^5)
U87
Day
E
Octyl α-KG (μM)
0
400
800
F
Octyl (R)-2HG (μM)
G
Octyl (S)-2HG (μM)
H
Glc, IDH1(WT)
Glc, IDH1(R132H)
Gal, IDH1(WT)
Gal, IDH1(R132H)
I
Glc, IDH1(+/+)
Glc, IDH1(R132H/+)
Gal, IDH1(+/+)
Gal, IDH1(R132H/+)
J
IDH1(WT)
IDH1(R132H)
NS
Control RNAi
ATP5B RNAi
K
WI-38
Vehicle
Octyl (R)-2HG
Octyl (S)-2HG
Octyl α-KG
L
HEK293
M
Jurkat
N
A549

Figure S4, related to Figure 4. Cells with ATP5B knockdown, octyl α-KG or octyl 2-HG treatment, or IDH mutations exhibit decreased viability and proliferation rate.
(A) HCT 116 IDH1(R132H/+) cells exhibit decreased viability upon glucose starvation. Cells were cultured in glucose-free, galactose-containing medium.
(B) Octyl citrate treated U87 cells do not exhibit altered viability upon glucose starvation. Cells were cultured in galactose medium. Octyl citrate and octyl (*R*)-2HG were each at 800 μM.
(C) mTOR complex I activity is decreased in U87 cells treated with octyl 2-HG through both an AMPK-independent and AMPK-depenent manner. Cells were cultured in glucose-free, galactose-containing medium. Phospho-raptor (S792) is not clearly modulated upon octyl 2-HG treatment, suggesting that raptor phosphorylation may not play a major role in 2-HG mediated mTOR signaling in U87 cells, consistent with results using oligomycin treatment.
(D) ATP5B knockdown decreases the growth rate of U87 cells even in glucose-containing medium.
(E-G) U87cells exhibit decreased growth rate upon treatment with octyl α-KG (E), octyl *(R)*-2HG (F), or octyl *(S)*-2HG (G) in glucose-free medium (galactose medium). In glucose-containing medium growth rate was also reduced albeit to a lesser extent (not shown).
(H) Compared to U87/IDH(WT) cells, U87/IDH1(R132H) cells exhibit decreased growth rate both in glucose-containing (Glc) and in glucose-free, galactose-contaning (Gal) media.
(I) HCT 116 IDH1(R132H/+) cells present decreased proliferation both in glucose-containing (Glc) and in glucose-free, galactose-containing (Gal) media.
(J) Reduced growth in U87/IDH1(R132H) cells is ATP synthase dependent.
(K-N) WI-38, HEK293,Jurkat, A549 cells also exhibit decreased growth rate upon treatment with octyl 2-HG or octyl α-KG in glucose-containing medium.
*****P* < 0.0001, ****P* < 0.001, ***P* < 0.01, **P* < 0.05; NS, *P* > 0.05; unpaired *t*-test, two-tailed, two-sample unequal variance. Mean ± s.d. is plotted in all cases. All growth curve results were replicated in at least two independent experimens.

Supplemental Experimental Procedures

Lifespan analysis

Lifespan experiments were performed as previously described (Chin et al., 2014). Lifespan assays were conducted at 20 °C on solid nematode growth media (NGM) using standard protocols and were replicated in at least two independent experiments. *C. elegans* were synchronized by performing either a timed egg lay (Sutphin and Kaeberlein, 2009) or an egg preparation (lysing ~100 gravid worms in 70 µl M9 buffer (Brenner, 1974), 25 µl bleach (10% sodium hypochlorite solution) and 5 µl 10 N NaOH). L4 or young adult animals were picked onto NGM assay plates containing 1.5% dimethyl sulfoxide (DMSO; Sigma, D8418), 49.5 µM 5-fluoro-2′-deoxyuridine (Sutphin and Kaeberlein, 2009)(FUDR; Sigma, F0503), and D-2-HG (Sigma, H8378), L-2-HG (Sigma, 90790), α-KG (Sigma, K1128), or vehicle control (H_2O). FUDR was included to prevent progeny production. All compounds were mixed into the NGM media after autoclaving and before solidification of the media. Assay plates were seeded with OP50. For RNAi experiments, NGM assay plates also contained 1 mM isopropyl-b-D-thiogalactoside (IPTG) and 50 µg/mL ampicillin, and were seeded with the appropriate RNAi feeding clone (Thermo Scientific / OpenBiosystems). The *C. elegans* TOR (*let-363*) RNAi clone was obtained from Joseph Avruch (MGH/Harvard). Worms were moved to new assay plates every 4 days (to ensure sufficient food was present at all times and to reduce the risk of mould contamination). To assess the survival of the worms, the animals were prodded with a platinum wire every 2–3 days, and those that failed to respond were scored as dead. Animals were assigned randomly to the experimental groups. Worms that ruptured, bagged (that is, exhibited internal progeny hatching), or crawled off the plates were censored. Lifespan data were analysed using GraphPad Prism; *P* values were calculated using the log-rank (Mantel–Cox) test unless stated otherwise.

Target identification using drug affinity responsive target stability (DARTS)

DARTS was performed as described (Lomenick et al., 2009; Lomenick et al., 2011). Briefly, U87 cells were lysed in M-PER buffer (Thermo Scientific, 78501) with the addition of protease (Roche, 11836153001) and phosphatase (50 mM NaF, 2 mM Na_3VO_4) inhibitors. Chilled TNC buffer (50 mM Tris-HCl pH 8.0, 50 mM NaCl, 10 mM $CaCl_2$) was added to the lysate, and protein concentration of the solution was measured on an aliquot by the BCA Protein Assay kit (Pierce, 23227). The remaining lysate was then incubated with vehicle control (H_2O) or varying concentrations of 2-HG or α-KG for 0.5 h at room temperature. The samples were then subjected to Pronase (Roche, 10165921001) digestions (5 min at room temperature) that were stopped by addition of SDS loading buffer and immediate heating (95 °C, 5 min). Samples were subjected to SDS-PAGE on 4-12% Bis-Tris gradient gel (Invitrogen, NP0322BOX), and Western blotting was carried out with antibodies against ATP5B (Sigma, AV48185) or GAPDH (Santa Cruz, SC25778).

Cell Culture

U87 cells were cultured in glucose-free DMEM (Life technologies, 11966-025) supplemented with 10% fetal bovine serum (FBS) and 10 mM glucose or 10 mM galactose when indicated. IDH1(R132H) and IDH1(WT) expressing U87 cells were as reported (Li et al., 2013). U87 cells are unable to utilize ketone bodies for energy (Maurer et al., 2011; Seyfried et al., 2011). HCT 116 IDH1(R132H/+) and parental control cells (Horizon Discovery, HD 104-013) were cultured in RPMI (Life technologies, 11875-093) supplemented with 10% FBS or DMEM (Life technologies, 11966-025) supplemented with 10% FBS and

10 mM glucose or 10 mM galactose. Normal human diploid fibroblasts WI-38 (ATCC, CCL-75) were cultured with EMEM (ATCC, 30-2003) supplemented with 10% FBS. HEK 293, A549, and HeLa cells were cultured with DMEM (Life technologies, 11966-065) supplemented with 10% FBS. Jurkat cells were cultured in RPMI supplemented with 10% FBS. All cells were cultured at 37°C and 5% CO2. Cells were transfected with indicated siRNA using DharmaFECT 1 Transfection Reagent by following the manufacturer's instructions. Knockdown efficiency was confirmed by Western blotting.

Assay for cellular ATP levels

For Figure S2A, U87 cells were seeded in 96-well plates at 2 x 10^4 cells per well and treated with indicated compound for 2 h in triplicate. ATP levels were measured using the CellTiter-Glo luminescent ATP assay (Promega, G7572); luminescence was read using Analyst HT (Molecular Devices). To confirm that the number of cells was consistent between treatments, cell lysates were further subjected to dsDNA staining using QuantiFluor dsDNA system (Promega). Statistical analysis was performed using GraphPad Prism (unpaired *t*-test).

Determination of ATP/ADP ratio

For Figure 2D and Figure S2B, U87 cells were seeded in 96-well plates at 10^4 cells/well and treated with indicated compound for 24 h. ATP/ADP ratios were measured by using EnzyLight ADP/ATP Ratio Assay Kit (BioAssay Systems); luminescence was read using Synergy H1m (BioTek). For Figure 3A, ATP and ADP levels were measured by LC-MS.

Measurement of oxygen consumption rates (OCR) and extracellular acidification rates (ECAR)

OCR and ECAR measurements were made using a Seahorse XF-24 analyzer (Seahorse Bioscience)(Wu et al., 2007). U87 cells were seeded in Seahorse XF-24 cell culture microplates at 50,000 cells per well in DMEM supplemented with 10% FBS and either 10 mM glucose or 10 mM galactose, and incubated O/N at 37 °C in 5% CO_2. Treatment with octyl α-KG, octyl (*R*)-2HG, octyl (*S*)-2HG, or DMSO (vehicle control) was for 1 h. Cells were washed in unbuffered DMEM (pH 7.4, 10 mM glucose) immediately prior to measurement, and maintained in this buffer with indicated concentrations of compound. OCR or ECAR were measured 3 times under basal conditions and normalized to protein concentration per well. Statistical analysis was performed using GraphPad Prism (unpaired *t*-test, two-tailed, two-sample unequal variance).

Isolation of mitochondria from mouse liver

Animal studies were performed under approved UCLA animal research protocols. Mitochondria from 3-month-old C57BL/6 mice were isolated as described (Rogers et al., 2011). Briefly, livers were extracted, minced at 4 °C in MSHE+BSA (70 mM sucrose, 210 mM mannitol, 5 mM HEPES, 1 mM EGTA, and 0.5% fatty acid free BSA, pH 7.2), and rinsed several times to remove blood. All subsequent steps were performed on ice or at 4 °C. The tissue was disrupted in 10 volumes of MSHE+BSA with a glass Dounce homogenizer (5-6 strokes) and the homogenate was centrifuged at 800 x *g* for 10 min to remove tissue debris and nuclei. The supernatant was decanted through a cell strainer and centrifuged at 8,000 x *g* for 10 min. The dark mitochondrial pellet was resuspended in MSHE+BSA and re-centrifuged at 8,000 x *g* for 10 min. The final mitochondrial pellets were used for various assays as described below.

Measurement of mitochondrial respiration

Mitochondrial respiration was analyzed using isolated mouse liver mitochondria (see (Brand and Nicholls, 2011) and refs therein). Mitochondria were isolated from mouse liver as described above. The final mitochondrial pellet was resuspended in 30 µL of MAS buffer (70 mM sucrose, 220 mM mannitol, 10 mM KH2PO4, 5 mM MgCl2, 2 mM HEPES, 1 mM EGTA, and 0.2% fatty acid free BSA, pH 7.2).
Isolated mitochondrial respiration was measured by running coupling and electron flow assays as described (Rogers et al., 2011). For the coupling assay, 5 µg of mitochondria in complete MAS buffer (MAS buffer supplemented with 10 mM succinate and 2 µM rotenone) were seeded into a XF24 Seahorse plate by centrifugation at 2,000 x *g* for 20 min at 4 °C. Just before the assay, the mitochondria were supplemented with complete MAS buffer for a total of 500 µL (with octanol or octyl 2-HG), and warmed at 37 °C for 30 min before starting the oxygen consumption rate measurements. Mitochondrial respiration begins in a coupled State 2; State 3 is initiated by 2 mM ADP; State 4o (oligomycin-insensitive, that is, complex V independent) is induced by 2.5 µM oligomycin and State 3u (FCCP-uncoupled maximal respiratory capacity) by 4 µM FCCP. Finally, 1.5 µg/mL antimycin A was injected at the end of the assay. For the electron flow assay, the MAS buffer was supplemented with 10 mM sodium pyruvate, 2 mM malate and 4 µM FCCP, and the mitochondria are seeded the same way as described for the coupling assay. After basal readings, the sequential injections were as follows: 2 µM rotenone (complex I inhibitor), 10 mM succinate (complex II substrate), 4 µM antimycin A (complex III inhibitor), and 10 mM/100 µM ascorbate/tetramethylphenylenediamine (complex IV substrate).
There is no known transporter for 2-HG in the mitochondria; transport of α-KG by the α-KG/malate shuttle is rate limiting. If unmodified 2-HG or α-KG were to be used to inhibit ATP synthase, an excessively longer incubation time – which jeopardizes mitochondrial integrity – would be required to allow intra-mitochondrial 2-HG and α-KG to accumulate. Octyl esters of 2-HG and α-KG allow rapid uptake across the intact inner mitochondrial membrane, upon which 2-HG or α-KG is produced through in situ hydrolysis by intramitochondrial esterases.

Submitochondrial particle (SMP) ATPase assay

ATP hydrolysis by ATP synthase was measured using submitochondrial particles (see (Alberts, 1994) and refs therein). Mitochondria were isolated from mouse liver as described above. The final mitochondrial pellet was resuspended in buffer A (250 mM sucrose, 10 mM Tris-HCl, 1 mM ATP, 5 mM $MgCl_2$, and 0.1 mM EGTA, pH 7.4) at 10 µg/µL, subjected to sonication on ice (Fisher Scientific Model 550 Sonic Dismembrator; medium power, alternating between 10 s intervals of sonication and resting on ice for a total of 60 s of sonication), and then centrifuged at 18,000 x *g* for 10 min at 4 °C. The supernatant was collected and centrifuged at 100,000 x *g* for 45 min at 4 °C. The final pellet (submitochondrial particles) was resuspended in buffer B (250 mM sucrose, 10 mM Tris-HCl, and 0.02 mM EGTA, pH 7.4).
Submitochondrial particles were diluted to 2.75 ng/µl in reaction buffer (40 mM Tris pH 7.5, 0.1 mg/mL BSA, 3 mM $MgCl_2$), and then incubated with either vehicle or drug for 45 min at room temperature. To start the ATPase reaction, ATP was added to a final concentration of 125 µM. The amount of phosphate produced after 6 min was determined by the Malachite Green Phosphate Assay Kit (BioAssay POMG-25H) and was used to calculate ATPase activity. Oligomycin (Cell signaling, 9996) was used as a positive control for the assay. Unmodified 2-HG and α-KG were used in the SMP assay since submitochondrial particles are essentially inside-out mitochondria that allow the otherwise inner mitochondrial membrane components access to non-membrane permeable molecules (Alberts, 1994).

Complex IV activity assay

Complex IV activity was assayed using the MitoTox OXPHOS Complex IV Activity Kit (Abcam, ab109906), according to the manufacturer's instructions.

Assay for ADP import

Freshly prepared mice liver mitochondria were suspended at 1 μg/μL in medium consisting of 220 mM mannitol, 70 mM sucrose, 2 mM HEPES, 2.74 μM antimycin A, 5 μM rotenone, 1 mM EGTA, and 10 mM potassium phosphate buffer, pH 7.4. The mitochondria suspension was incubated with designated drug for 30 min in 37 ℃. After incubation, the suspension was transferred to ice for 10 min incubation. Afterwards, 100 μM [^{3}H]ADP (specific radioactivity, 185 kBq/pmol) was added, and the mixture was immediately vortexed and incubated for 20 s on ice. The reaction was terminated by addition of 10 μM carboxyatractyloside, and the mixture was centrifuged at 10,000 g for 10 min at 4 ℃. After centrifuge, the supernatant was collected for reading and the pellet was washed twice with the same medium supplemented with 10 μM carboxyatractyloside. After washing, the pellet was lysed by the addition of 0.2 ml of 1% SDS. The radioactivity of the lysate and supernatant was determined by TRI-CARB 2300 TR liquid scintillation analyzer. The ADP-ATP translocation rate was determined by the ratio of the pellet versus the sum reading of the pellet and supernatant.

Assay for mitochondria membrane potential

Mitochondrial membrane potential was determined using the MitoPT TMRM kit (ImmunoChemistry, #9105). Readings were normalized to cell number.

Assay for mammalian TOR (mTOR) pathway activity

mTOR pathway activity in cells treated with octyl 2-HG or oligomycin was determined by the levels of phosphorylation of known mTOR substrates, including S6K (T389), 4E-BP1 (S65), AKT (S473), and ULK1 (S757) (Pullen and Thomas, 1997; Burnett et al., 1998; Brunn et al., 1997; Choo et al., 2008; Sengupta et al., 2010; Gingras et al., 2001; Sarbassov et al., 2005; Kim et al., 2011). Specific antibodies used: phospho (P)-S6K T389 (Cell Signaling, 9234), S6K (Cell Signaling, 9202S), P-4E-BP1 S65 (Cell Signaling, 9451S), 4E-BP1 (Cell Signaling, 9452S), P-AKT S473 (Cell Signaling, 4060S), AKT (Cell Signaling, 4691S), P-ULK1 S757 (Cell Signaling, 6888), ULK1 (Cell Signaling, 4773S), P-AMPKα T172 (Cell Signaling, 2535S), AMPKα (Cell Signaling, 2532S), P-Raptor S792 (Cell Signaling, 2083S), Raptor (Cell Signaling, 2280S), and GAPDH (Santa Cruz Biotechnology, 25778).

Synthesis of octyl esters of α-KG, 2-HG, and citrate

Synthesis of 1-octyl α-KG has recently been published by GD and MEJ (Jung and Deng, 2012). Syntheses of octyl (*S*)-2HG and octyl (*R*)-2HG were carried out as reported (Albert et al., 1987; Xu et al., 2011) with modifications below.

Synthesis of 1-Octyl (*S*) 2-hydroxypentanedioate (Octyl (*S*)-2HG)

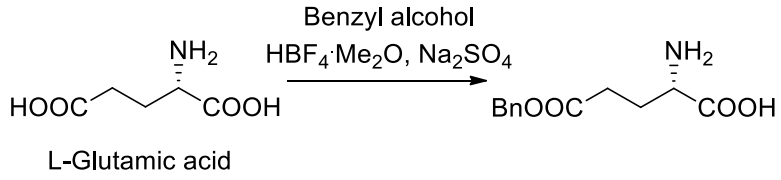

(*S*)-2-Amino-5-(benzyloxy)-5-oxopentanoic acid: L-Glutamic acid (2.0 g, 13.6 mmol) and anhydrous sodium sulfate (2.0 g) was dissolved in benzyl alcohol (25 mL), and then tetrafluoroboric acid diethyl ether

complex (3.7 mL, 27.2 mmol) was added. The suspended mixture was stirred at 21 °C overnight. Anhydrous THF (75 mL) was added to the mixture and it was filtered through a thick pad of activated charcoal. Anhydrous triethylamine (4.1 mL) was added to the clear filtrate to obtain a milky white slurry. Upon trituration with ethyl acetate (100 mL), the monoester monoacid precipitated. It was collected, washed with additional ethyl acetate (2 X 10 mL), and dried in vacuo to give the desired product (*S*)-2-amino-5-(benzyloxy)-5-oxopentanoic acid (3.07 g, 95%) as a white solid. ^{1}H NMR (500 MHz, Acetic acid-d_4): δ 7.41 – 7.25 (m, 5H), 5.14 (s, 2H), 4.12 (m, 1H), 2.75 – 2.60 (m, 2H), 2.27 (m, 2H). ^{13}C NMR (125 MHz, Acetic acid-d_4): δ 174.6, 174.4, 136.9, 129.5, 129.2, 129.1, 67.7, 55.0, 30.9, 26.3.

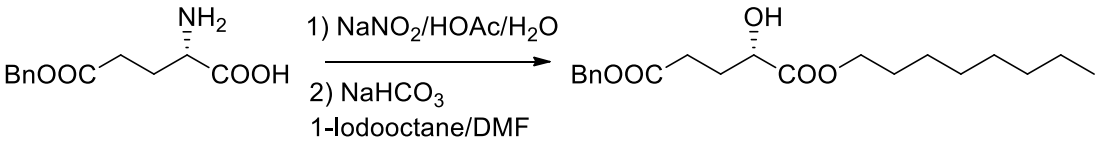

(*S*)-5-Benzyl 1-octyl 2-hydroxypentanedioate: To a solution of (*S*)-2-amino-5-(benzyloxy)-5-oxopentanoic acid (1.187 g, 5.0 mmol) in H_2O (25 mL) and acetic acid (10 mL) cooled to 0 ^{o}C was added slowly a solution of aqueous sodium nitrite (1.07 g in 15 mL H_2O). The reaction mixture was allowed to warm slowly to room temperature and was stirred overnight. The mixture was concentrated. The resulting residue was dissolved in DMF (15 mL) and $NaHCO_3$ (1.26 g, 15 mmol) and 1-iodooctane (1.84 mL, 10 mmol) were added to the mixture. The mixture was stirred at 21 °C overnight and then extracted with ethyl acetate (3 × 50 mL). The combined organic phase was washed with water and brine and dried over anhydrous $MgSO_4$. Flash column chromatography on silica gel eluting with 7/1 hexanes/ethyl acetate gave the desired mixed diester (*S*)-5-benzyl 1-octyl 2-hydroxypentanedioate (0.785 g, 45%) as a colorless oil. ^{1}H NMR (500 MHz, $CDCl_3$): δ 7.37 – 7.28 (m, 5H), 5.12 (s, 2H), 4.26 – 4.19 (m, 1H), 4.16 (t, *J* = 6.8 Hz, 2H), 3.11 (m, 1H), 2.61 – 2.46 (m, 2H), 2.26 – 2.14 (m, 1H), 1.95 (m, 1H), 1.71 – 1.57 (m, 2H), 1.39 – 1.20 (m, 10H), 0.88 (t, *J* = 6.9 Hz, 3H). ^{13}C NMR (125 MHz, $CDCl_3$): δ 174.6, 172.8, 135.8, 128.4, 128.1, 128.0, 69.3, 66.2, 65.8, 31.6, 29.6, 29.2, 29.0 (2C's), 28.4, 25.6, 22.5, 13.9.

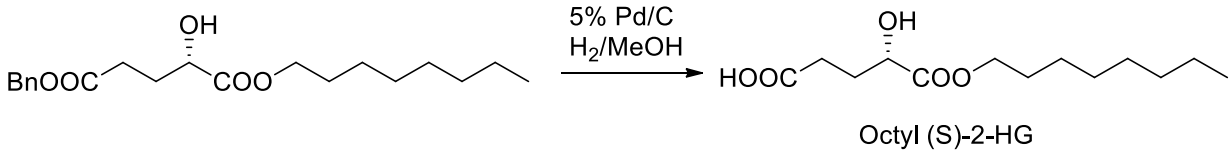

Octyl (S)-2-HG

1-Octyl (*S*) 2-hydroxypentanedioate (octyl (*S*)-2-hydroxyglutarate; octyl (*S*)-2HG): To a solution of (*S*)-5-benzyl 1-octyl 2-hydroxypentanedioate (0.71 g, 2.0 mmol) in MeOH (50 mL) was added 5% Pd/C (80 mg). Over the mixture was passed argon and then the argon was replaced with hydrogen and the mixture was stirred vigorously for 1 h. The mixture was filtered through a thick pad of Celite and the organic phase was evaporated. The residue was purified via flash column chromatography on silica gel eluting with 25/1 CH_2Cl_2/MeOH to give octyl (*S*)-2HG (0.495 g, 48%) as a white solid. ^{1}H NMR (500 MHz, $CDCl_3$): δ 4.23 (dd, *J* = 8.0, 4.2 Hz, 1H), 4.16 (t, *J* = 6.8 Hz, 2H), 2.60 – 2.42 (m, 2H), 2.15 (m, 1H), 1.92 (m, 1H), 1.69 – 1.59 (m, 2H), 1.38 – 1.16 (m, 10H), 0.86 (t, *J* = 7.0 Hz, 3H). ^{13}C NMR (125 MHz, $CDCl_3$): δ 178.8, 174.8, 69.3, 66.1, 31.7, 29.4, 29.1 (2C's), 28.9, 28.4, 25.7, 22.5, 14.0.

Synthesis of 1-Octyl (*R*) 2-hydroxypentanedioate (Octyl (*R*)-2HG)

The synthesis of the opposite enantiomer, i.e., Octyl (*R*)-2HG, was carried out by the exact same procedure starting with D-glutamic acid. The spectroscopic data was identical to that of the enantiomeric compounds.

Synthesis of 1-octyl citrate ester (Kotick, 1991; Weaver and Gilbert, 1997; Takeuchi et al., 1999)

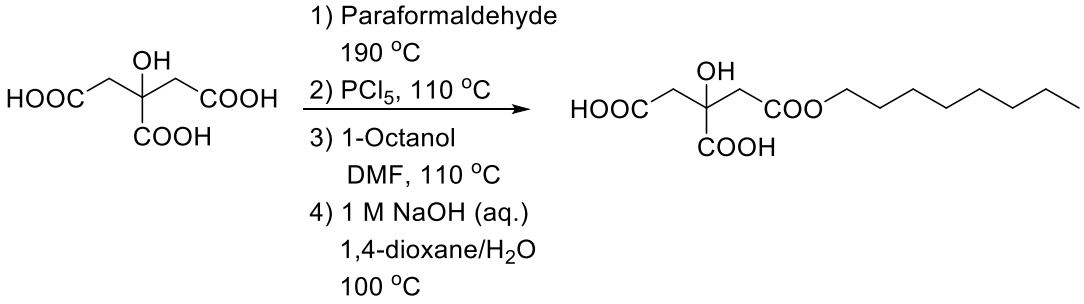

The mixture of citric acid (3.862 g, 0.02 mol) and paraformaldehyde (1.276 g, 0.04 mol) was stirred at 190 °C for 2 h. After cooling down to room temperature, the mixture was purified by flash column chromatography on silica gel eluting with 10/1 dichloromethane/methanol gave the desired methylene acetal of citric acid. The diacetic acid product (0.816 g, 4.0 mmol) and phosphorus (V) chloride (0.850 g, 4.0 mmol) were stirred with heating from room temperature to 110 °C in 1 h and kept at 110 °C until there was no further emission of hydrogen chloride. After cooling the mixture to room temperature, the phosphorus oxychloride was evaporated under vacuum. The residue was dissolved in ethyl acetate, the mixture was filtered, and the organic phase was evaporated. The resulting residue was dissolved in DMF (3.0 mL) and 1-octanol (1.89 mL, 0.012 mol) was added. The mixture was heated to 110 °C for 3 h and then extracted with ethyl acetate (3 × 50 mL). The combined organic phase was washed with water and brine and dried over anhydrous $MgSO_4$. Flash column chromatography on silica gel eluting with 15/1 dichloromethane/methanol gave the mono-octyl methylene acetal of citric acid ester (0.652 g, 52%) as a colorless oil. This mono-octyl ester (0.2576 g, 0.814 mmol) was dissolved in 1,4-dioxane (3.0 mL) and H_2O (3.0 mL). An aqueous solution of NaOH (1.0 M, 0.82 mL) was added to the mixture and the temperature was raised to 100 °C for 2 h. After cooling down the mixture to room temperature, an aqueous solution of NaOH (0.2 M, 10 mL) was added. The mixture was extracted with ethyl acetate (3 X 10mL) and the aqueous phase was acidified with 1.0 M aqueous HCl to pH 1. The acidified aqueous layer was extracted with ethyl acetate (3 X 30 mL), and the combined organic phases were washed with water and brine and dried over anhydrous $MgSO_4$. Flash column chromatography on silica gel, eluting with 10/1 dichloromethane/methanol, gave the 1-octyl citrate ester as an oil (0.183 g, 74%). ^{1}H NMR (500 MHz, $CDCl_3$) δ 10.55 (s, 2H), 4.05 (t, J = 6.5 Hz, 2H), 2.88 (m, 4H), 1.57 (m, 2H), 1.23 (m, 10H), 0.84 (t, J = 6.2 Hz, 3H). ^{13}C NMR (125 MHz, $CDCl_3$) δ 177.63, 174.68, 170.08, 72.82, 65.45, 42.81, 42.69, 31.63, 29.03, 29.01, 28.25, 25.66, 22.48, 13.92.

Supplemental References

Albert, R., Danklmaier, J., Honig, H., and Kandolf, H. (1987). A Simple and Convenient Synthesis of Beta-Aspartates and Gamma-Glutamates. Synthesis-Stuttgart, 635-637.

Alberts, B. (1994). Molecular biology of the cell. (New York: Garland Pub.).

Brand, M.D., and Nicholls, D.G. (2011). Assessing mitochondrial dysfunction in cells. Biochem J *435*, 297-312.

Brenner, S. (1974). The genetics of Caenorhabditis elegans. Genetics *77*, 71-94.

Brunn, G.J., Hudson, C.C., Sekulic, A., Williams, J.M., Hosoi, H., Houghton, P.J., Lawrence, J.C., Jr., and Abraham, R.T. (1997). Phosphorylation of the translational repressor PHAS-I by the mammalian target of rapamycin. Science *277*, 99-101.

Burnett, P.E., Barrow, R.K., Cohen, N.A., Snyder, S.H., and Sabatini, D.M. (1998). RAFT1 phosphorylation of the translational regulators p70 S6 kinase and 4E-BP1. Proc Natl Acad Sci U S A *95*, 1432-1437.

Choo, A.Y., Yoon, S.O., Kim, S.G., Roux, P.P., and Blenis, J. (2008). Rapamycin differentially inhibits S6Ks and 4E-BP1 to mediate cell-type-specific repression of mRNA translation. Proc Natl Acad Sci U S A *105*, 17414-17419.

Fendt, S.M., Bell, E.L., Keibler, M.A., Olenchock, B.A., Mayers, J.R., Wasylenko, T.M., Vokes, N.I., Guarente, L., Vander Heiden, M.G., and Stephanopoulos, G. (2013). Reductive glutamine metabolism is a function of the alpha-ketoglutarate to citrate ratio in cells. Nat Commun *4*, 2236.

Gingras, A.C., Raught, B., Gygi, S.P., Niedzwiecka, A., Miron, M., Burley, S.K., Polakiewicz, R.D., Wyslouch-Cieszynska, A., Aebersold, R., and Sonenberg, N. (2001). Hierarchical phosphorylation of the translation inhibitor 4E-BP1. Genes Dev *15*, 2852-2864.

Jung, M.E., and Deng, G. (2012). Synthesis of the 1-monoester of 2-ketoalkanedioic acids, for example, octyl alpha-ketoglutarate. J Org Chem *77*, 11002-11005.

Kim, J., Kundu, M., Viollet, B., and Guan, K.L. (2011). AMPK and mTOR regulate autophagy through direct phosphorylation of Ulk1. Nat Cell Biol *13*, 132-141.

Kotick, M.P. (1991). Method for regioselective preparation of 1- or 2-monoalkyl citrates as surfactants. U.S. Patent *US5049699*, A19910917.

Li, S., Chou, A.P., Chen, W., Chen, R., Deng, Y., Phillips, H.S., Selfridge, J., Zurayk, M., Lou, J.J., Everson, R.G., et al. (2013). Overexpression of isocitrate dehydrogenase mutant proteins renders glioma cells more sensitive to radiation. Neuro Oncol *15*, 57-68.

Lomenick, B., Jung, G., Wohlschlegel, J.A., and Huang, J. (2011). Target identification using drug affinity responsive target stability (DARTS). Curr Protoc Chem Biol *3*, 163-180.

Maurer, G.D., Brucker, D.P., Bahr, O., Harter, P.N., Hattingen, E., Walenta, S., Mueller-Klieser, W., Steinbach, J.P., and Rieger, J. (2011). Differential utilization of ketone bodies by neurons and glioma cell lines: a rationale for ketogenic diet as experimental glioma therapy. BMC Cancer *11*, 315.

Pullen, N., and Thomas, G. (1997). The modular phosphorylation and activation of p70s6k. FEBS Lett *410*, 78-82.

Rogers, G.W., Brand, M.D., Petrosyan, S., Ashok, D., Elorza, A.A., Ferrick, D.A., and Murphy, A.N. (2011). High throughput microplate respiratory measurements using minimal quantities of isolated mitochondria. PLoS One *6*, e21746.

Sarbassov, D.D., Guertin, D.A., Ali, S.M., and Sabatini, D.M. (2005). Phosphorylation and regulation of Akt/PKB by the rictor-mTOR complex. Science *307*, 1098-1101.

Sengupta, S., Peterson, T.R., and Sabatini, D.M. (2010). Regulation of the mTOR complex 1 pathway by nutrients, growth factors, and stress. Mol Cell *40*, 310-322.

Seyfried, T.N., Kiebish, M.A., Marsh, J., Shelton, L.M., Huysentruyt, L.C., and Mukherjee, P. (2011). Metabolic management of brain cancer. Biochim Biophys Acta *1807*, 577-594.

Sutphin, G.L., and Kaeberlein, M. (2009). Measuring Caenorhabditis elegans life span on solid media. J Vis Exp.

Takeuchi, Y., Nagao, Y., Toma, K., Yoshikawa, Y., Akiyama, T., Nishioka, H., Abe, H., Harayama, T., and Yamamoto, S. (1999). Synthesis and siderophore activity of vibrioferrin and one of its diastereomeric isomers. Chemical & Pharmaceutical Bulletin *47*, 1284-1287.

Weaver, R., and Gilbert, I.H. (1997). The design and synthesis of nucleoside triphosphate isosteres as potential inhibitors of HIV reverse transcriptase. Tetrahedron *53*, 5537-5562.

Wu, M., Neilson, A., Swift, A.L., Moran, R., Tamagnine, J., Parslow, D., Armistead, S., Lemire, K., Orrell, J., Teich, J., et al. (2007). Multiparameter metabolic analysis reveals a close link between attenuated mitochondrial bioenergetic function and enhanced glycolysis dependency in human tumor cells. Am J Physiol Cell Physiol *292*, C125-136.